



PERGAMON

Journal of Geodynamics 35 (2003) 521–539

---

---

JOURNAL OF  
**GEODYNAMICS**

---

---

www.elsevier.com/locate/jog

# Influence of soil consolidation and thermal expansion effects on height and gravity variations

C. Romagnoli<sup>a</sup>, S. Zerbini<sup>b,\*</sup>, L. Lago<sup>b</sup>, B. Richter<sup>c</sup>, D. Simon<sup>c</sup>, F. Domenichini<sup>b</sup>,  
C. Elmi<sup>a</sup>, M. Ghirotti<sup>a</sup>

<sup>a</sup>*Dipartimento di Scienze della Terra e Geologico Ambientali, Università di Bologna, Piazza di Porta San Donato 1, 40127 Bologna, Italy*

<sup>b</sup>*Dipartimento di Fisica, Università di Bologna, Italy*

<sup>c</sup>*Bundesamt fuer Kartographie und Geodaesie, Frankfurt am Main, Germany*

---

## Abstract

The daily GPS height series of the Medicina station were analyzed for the period July 1996–September 2001. The station is located in the middle Po Plain on fine-grained alluvial deposits. A seasonal oscillation in the order of 18 mm (peak-to-peak amplitude) is present in the data. This crustal deformation has been modeled by including variations in the atmospheric, oceanic and hydrologic mass. The vertical positions can also be affected significantly by soil consolidation. Geotechnical parameters derived by in situ tests and laboratory analyses of the clayey soil collected at Medicina allowed the estimate of the soil settlement relevant to the seasonal oscillation of the surficial water table. Thermal expansion of the geodetic monument has to be taken into account in the case of high-precision vertical positioning. In this work models both for the soil consolidation and the thermal expansion effects are provided. The continuous gravity observations collected at Medicina by means of a superconducting gravimeter also exhibit a marked seasonal oscillation, which has been interpreted as the sum of loading and Newtonian attraction effects, as well as of the contribution due to soil consolidation. Especially the study concerning the soil consolidation effect has allowed a better insight on the seasonal vertical movements occurring at the Medicina station by providing quantitative information on soil behavior due to change of effective pressures. The results can be applied to those stations characterized by similar fine-grained soils and surficial hydrogeology.

© 2003 Elsevier Science Ltd. All rights reserved.

---

## 1. Introduction

The Department of Physics of the University of Bologna installed in mid 1996 at Medicina a permanent GPS (continuous GPS, CGPS) station to monitor crustal movements and, in parti-

---

\* Corresponding author. Tel.: +39-051-209-5019; fax: +39-051-209-5058.

E-mail address: zerbini@df.unibo.it (S. Zerbini).

cular, height variations because of the subsidence problem affecting wide sectors of the south-eastern Po Plain (Arca and Beretta, 1985; Fig. 1). Several environmental parameters are collected with the scope to provide significant information on the potential effects induced on height variations by phenomena of climatic origin. Air pressure, temperature, rainfall and water table are monitored continuously.

To get additional information on mass variations, a superconducting gravimeter (SG), belonging to the Bundesamt fuer Kartographie und Geodaesie of Frankfurt was installed in October 1996 to monitor continuously the variations of the gravity field. The SG is periodically controlled by means of absolute gravity measurements. The co-location of CGPS and SG allows the separation of the gravity potential signal due to mass redistribution from the geometric signal due to height changes/variations (Zerbini et al., 2001).

The picture in Fig. 2(a) describes the CGPS installation. The antenna is supported by a steel rod, specifically designed, screwed into the reference benchmark. This set-up, which is unchanged since the installation of the antenna, ensures the necessary accuracy in the determination and maintenance of the antenna's center of phase with respect to the ground benchmark. The benchmark is installed on the main pillar of the mobile satellite laser ranging (SLR) pad. The pillar, made of reinforced concrete, is founded 7 m deep into the ground whereas the SG was installed [Fig. 2(b)] about 600 m apart from the GPS system, in a temperature-controlled laboratory. The SG is set up on a concrete pier, founded 1 m deep into the ground.

Both the CGPS and SG data series exhibit significant seasonal fluctuations of comparable amplitude and phase. They have been attributed mainly to loading effects, as well as to mass effects in the case of gravity, caused by environmental parameters such as air pressure variations and the seasonal behavior of the hydrological cycle. Non-tidal oceanic contributions have been considered and modeled as well (Zerbini et al., 2001, 2002). Also at other CGPS stations seasonal oscillations in the CGPS data series are observed (Van Dam et al., 1997; Scherneck et al., 1998; Bingley et al., 2000; Dong et al., 2001). The understanding and modeling of these seasonal variations is important to guarantee the stability of the terrestrial reference frame on short time scales. It has been demonstrated that a refined modeling of the seasonal fluctuations requires the availability of continuous data series of several environmental parameters, which are oftentimes site-dependent (Zerbini et al., 2001, 2002).

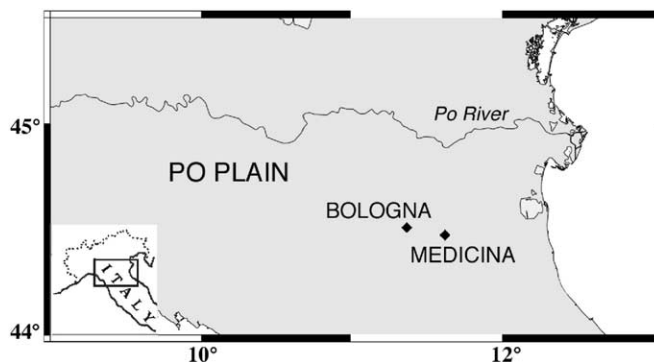


Fig. 1. Location of the Medicina station in the southern Po Plain.

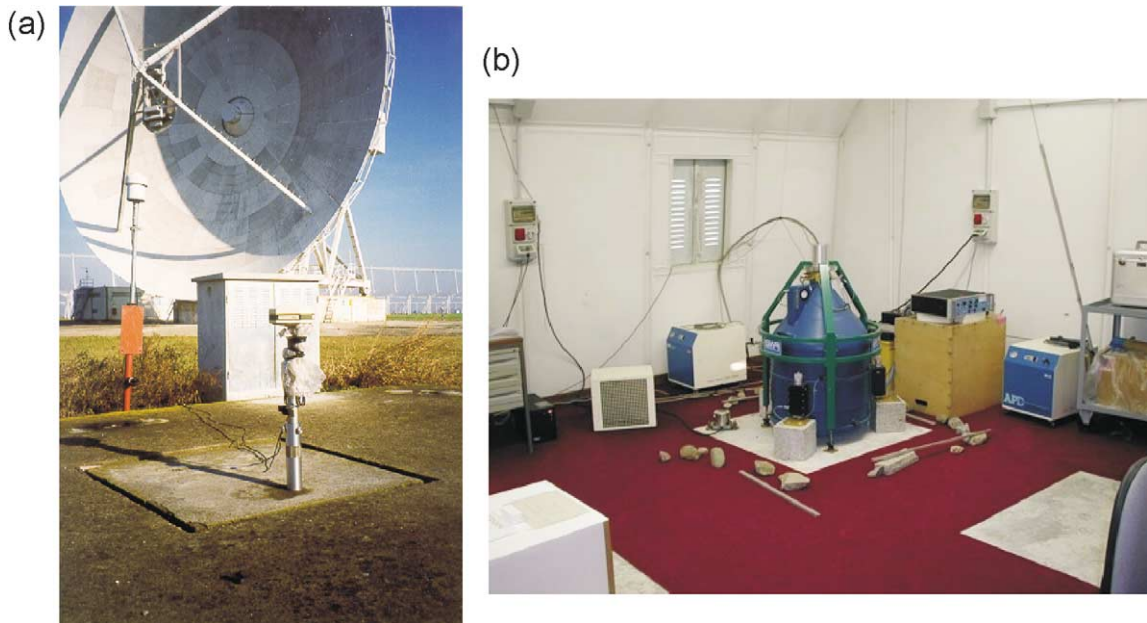


Fig. 2. (a) Installation of the CGPS antenna; (b) installation of the SG in the gravity laboratory.

The few millimeters level of accuracy presently achievable in the CGPS height determination suggests that it is worthwhile to investigate the effects of thermal expansion of the structures supporting the GPS antennas. These may amount up to several millimeters (peak-to-peak amplitude) depending upon the characteristics of the monumentation and of the structure (Wyatt, 1989). Bedrock thermal expansion has also been recently suggested as a possible component to seasonal effects (Dong et al., 2001). For monumentation founded on non-lithified sediments, soil consolidation effects should also be considered.

## 2. Height and gravity seasonal variations

Loading and, in the case of gravity, also mass effects influence height and gravity observations. These effects result from time-variable changes in the geographical redistribution of atmospheric, oceanic and hydrologic masses. These signals can induce peak-to-peak height variations up to a few cm and gravity fluctuations in the order of several  $\mu\text{Gal}$ , respectively and are mapped into the geodetic signal. Therefore, the seasonal oscillations must be identified by their nature and removed from the data series.

The high temporal resolution in the CGPS data allows the correlation of the observed seasonal fluctuations in the station heights to relevant variations of series of environmental parameters. This requires the availability of continuous measurements of several environmental parameters.

As a complementary method to space techniques, gravity measurements contribute to the realization of a vertical reference related to the geocenter. They provide an independent information on the occurrence of vertical crustal movements and on their dynamics. A SG is of major

importance to monitor the gravity field continuously, since absolute gravity observations are limited to relatively short time intervals, and gravity variations can hardly be deduced from such measurements. At present, the most accurate absolute and relative gravimeters are sensitive to height changes of less than 1 cm and therefore, provide information of comparable accuracy to that of CGPS.

### 2.1. Height variations

The Bernese software package version 4.2 (Beutler et al., 2001) was used for the GPS data analysis together with the IGS orbits. Five fiducial IGS stations in the European area whose coordinates and velocity field are given by the ITRF97 were adopted (Boucher et al., 1999). Earth's body tides effects are accounted for in the data analysis as well as site displacements due to ocean tide loading. Additional details on the GPS data analysis procedure can be found in Zerbinì et al. (2001, 2002). Fig. 3 shows the GPS daily height solutions smoothed by a 15-day window averaging and after a linear trend has been subtracted. This subsidence rate, over the time span considered, turns out to be of small magnitude ( $-0.6 \pm 0.1$  mm/year). A marked seasonal oscillation is present in the height series. The peak-to-peak amplitude is in the order of 18 mm. The maxima of the oscillation are in the summer period, in general during the month of August, while the minima occur during the winter season in the January–February time frame.

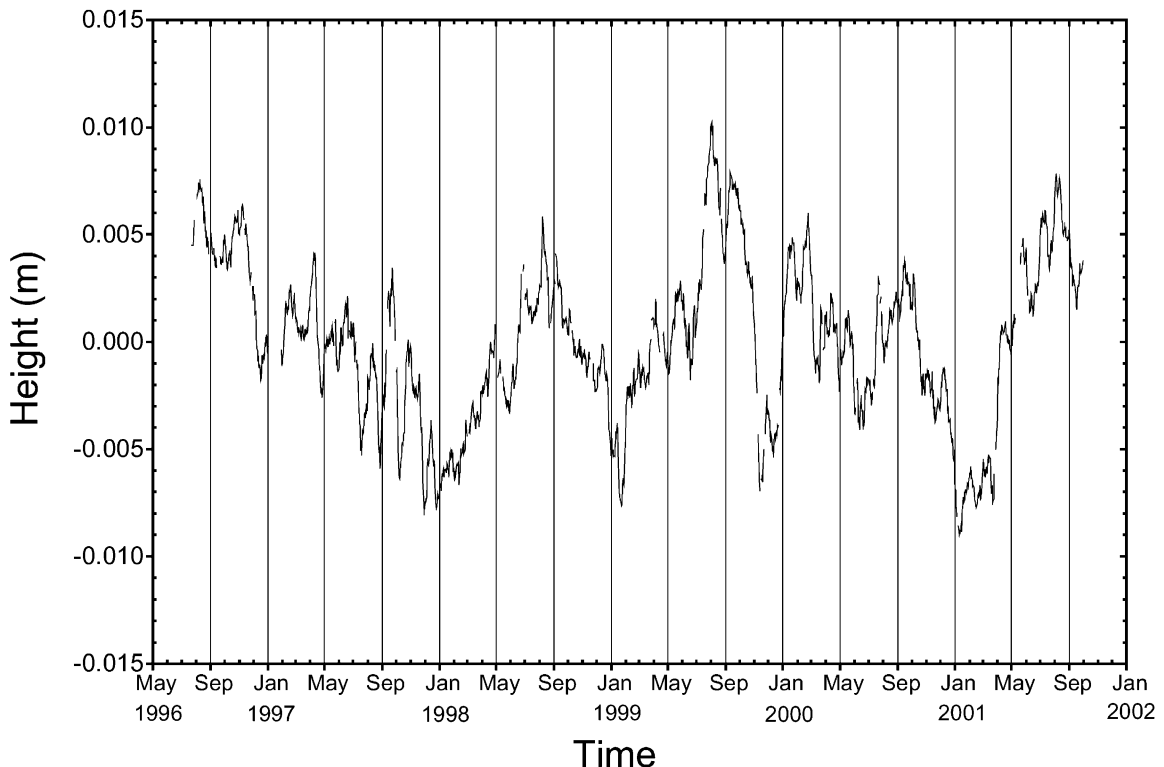


Fig. 3. Height residual series (linear trend removed) smoothed by a 15-day window averaging.

## 2.2. Gravity variations

The gravity data are collected with a 10 s sampling rate and then filtered to a 1 min rate. The data are pre-screened by means of the TSoft software package (Vauterin, 1998) and analyzed by using the ETERNA, version 3.30, software package (Wenzel, 1998). The tidal effects relevant to both the solid Earth and ocean loading components are accounted for in the analysis up to  $M_m$ . The long-period tides  $S_{sa}$  and  $S_a$  including the polar motion are estimated by adopting the theoretical value 1.16 for the elastic behavior of the Earth. The instrumental drift of the SG has been removed after intercomparison with absolute gravity (AG) measurements. Additional details on the data analysis procedure can be found in Zerbini et al. (2001). As common practice in gravity data analysis procedures, the effect of atmospheric pressure variations is removed from the data series by means of a transfer function between the local air pressure and gravity. Fig. 4 describes the gravity series. The data are daily averages of the SG recordings, smoothed by a 15-day window averaging, together with 15 AG measurements performed since the beginning of the SG observations. Daily averages were computed in order to have a direct comparison with the GPS daily series.

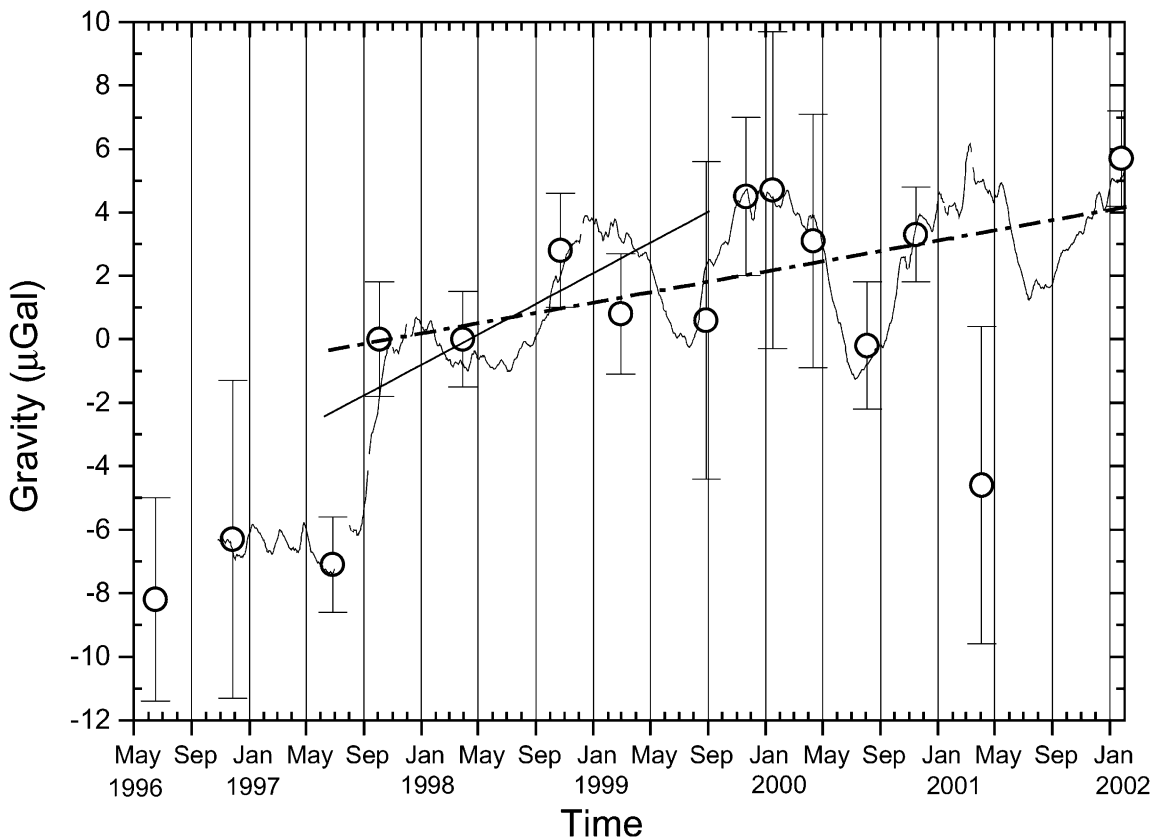


Fig. 4. Daily averages (solid line) of gravity values (SG), smoothed by a 15-day window averaging, corrected for air pressure, polar motion and tides. AG measurements (open circles) and linear trends.

As in the case of the height series, the gravity data show a remarkable seasonal oscillation of increasing amplitude, reaching peak-to-peak amplitude of 6  $\mu\text{Gal}$  during 2000. The phase has maxima around the end of December. The amplitude is quite comparable with that observed in the GPS heights and the phase is opposite to that of GPS heights as expected.

In addition, the gravity series is characterized by a sudden gravity increase occurred in mid 1997 and by the presence of linear trends as discussed in Zerbini et al. (2001, 2002). The rapid gravity change has been attributed by the authors to mass/density increase, likely associated with uprising of deep-seated salty waters in relation with local stress field changes. Two linear trends, computed after the occurrence of the gravity increase in mid 1997, are displayed in Fig. 4. They show that most of the contribution to the observed linear trend after mid 1997 ( $+0.97 \pm 0.03 \mu\text{Gal}/\text{year}$ ) comes from the gravity variation between 1998 and 1999 ( $+2.89 \pm 0.09 \mu\text{Gal}/\text{year}$ ). In fact, after second half of 1998, the positive trend in gravity is quite significantly reduced to  $+0.42 \pm 0.05 \mu\text{Gal}/\text{year}$ .

### 2.3. Seasonal loading and attraction effects on height and gravity

The present level of accuracy of both the CGPS heights (a few mm rms for daily solutions) and gravity series (less than 1  $\mu\text{Gal}$  for the long-term spectrum) requires thorough studies of physical processes characterized by a significant seasonal behavior. In the following a scheme of the data interpretation and modeling is provided. Starting with the standard analysis for both data types described above, and removing the long-term variations, the residual series are analyzed in order to decouple and model the remaining effects. For the height series, the non-tidal seasonal ocean loading effects and the loading caused by air pressure variations are estimated and removed. The thermal expansion of the monument and of the steel pole supporting the GPS antenna is estimated and removed, as well as the settlement of the clayey soil induced by the seasonal lowering of the water table (soil consolidation effect). Finally, the loading induced by the surficial hydrology has been taken into account by using a transfer function between the water table data and the height residuals. A more refined modeling of the surficial hydrological loading would require piezometric data from additional wells, which presently are not available.

As regards the gravity data, the contribution of the seasonal vertical air mass redistribution is subtracted (see Zerbini et al., 2001; Simon, in press). The soil consolidation and the non-tidal loading and Newtonian attraction effects due to the oceanic mass transport are estimated and removed from the data. After summing and removing all the mentioned contributions, one is left with the effect due to the surficial hydrology. As in the case of the height series, a transfer function between the local hydrological data series and the gravity residuals has been estimated and used to compute the gravity variations due to the seasonal hydrological behavior. This transfer function includes both the load and mass effects.

In the following, two effects are investigated which are strongly seasonal by their nature and usually not taken into account by standard analysis procedures. They are thermal expansion and soil consolidation. Whereas the latter acts on both instrumental setups, the thermal expansion effect on the pier on which the SG is installed is negligible because of the shallow foundation.

### 3. Thermal expansion

GPS antennas are, in general, mounted in different ways according to the local conditions of the station. As regards GPS height seasonal variations, we have investigated the effect of thermal expansion of the structure on which the antenna is set up. The potential contribution induced by the seasonal change in temperature has been derived by means of the following formula (Weast and Astle, 1982):

$$\Delta l = l_0 \times \alpha_t \times \Delta t^0 \quad (1)$$

where  $\Delta l$  is the length variation in meters due to thermal expansion,  $l_0$  is the initial length (m),  $\alpha_t$  is the thermal expansion coefficient ( $1/^\circ\text{C}$ ) and  $\Delta t^0$  is the air temperature variation ( $^\circ\text{C}$ ).

In Medicina, two components contributing to thermal expansion have been considered, the variation in the length of the reinforced concrete pillar, seven m deep into the ground, and the thermal dilatation of the 0.6 meter long steel pole supporting the antenna [see also Fig. 2(a)]. For the pillar as well as for the steel pole,  $\alpha_t$  has been assumed equal to  $12 \times 10^{-6}/^\circ\text{C}$  (Weast and Astle, 1982). By using daily means of the air temperature collected at the station, the variation in the length of the steel pole has been estimated according to the earlier formula. It turns out to be about 0.2 mm accounting for a seasonal temperature change in the order of  $30^\circ\text{C}$ . In order to estimate the variation in the length of the pillar, since the temperature variations in the 7 m layer of soil are not measured, a scaling factor of 4 has been assumed with respect to the observed air temperature variations. This limits the peak-to-peak seasonal temperature variations in the 7 m soil layer to a maximum of  $7\text{--}8^\circ\text{C}$ . Actually, this assumption can be substantiated by the results of repeated measurements of water temperature performed in phreatic wells around the area. These indicate that seasonal temperature variations in the order of  $7\text{--}8^\circ\text{C}$  are commonly observed in surficial groundwater, while smaller temperature fluctuations are recorded towards the bottom of the wells (within 10 m below the topographic surface) (Cremonini, 2002). The variation in the pillar length turns out to be about 0.7 mm. By adding the two contributions, a maximum seasonal height variation of the reference benchmark due to thermal expansion turns out to be in the order of 1 mm. Fig. 5 illustrates the seasonal change in length estimated for both the steel pole and the pillar.

### 4. Soil consolidation

Soil consolidation is a time-dependent physical process, which involves a void ratio reduction under loading conditions or increase of the effective pressures. These produce the expulsion of pore water, which leads to a soil settlement. According to the fundamental equation of Terzaghi (Terzaghi and Peck, 1974), the effective pressure  $p'$  is defined as

$$p' = p - u \quad (2)$$

where  $p$  is the total pressure and  $u$  is the neutral or pore pressure. The neutral pressure  $u$  acts in the water and in the solid in every direction with equal intensity and it is equal to

$$u = h \times \gamma_w \quad (3)$$

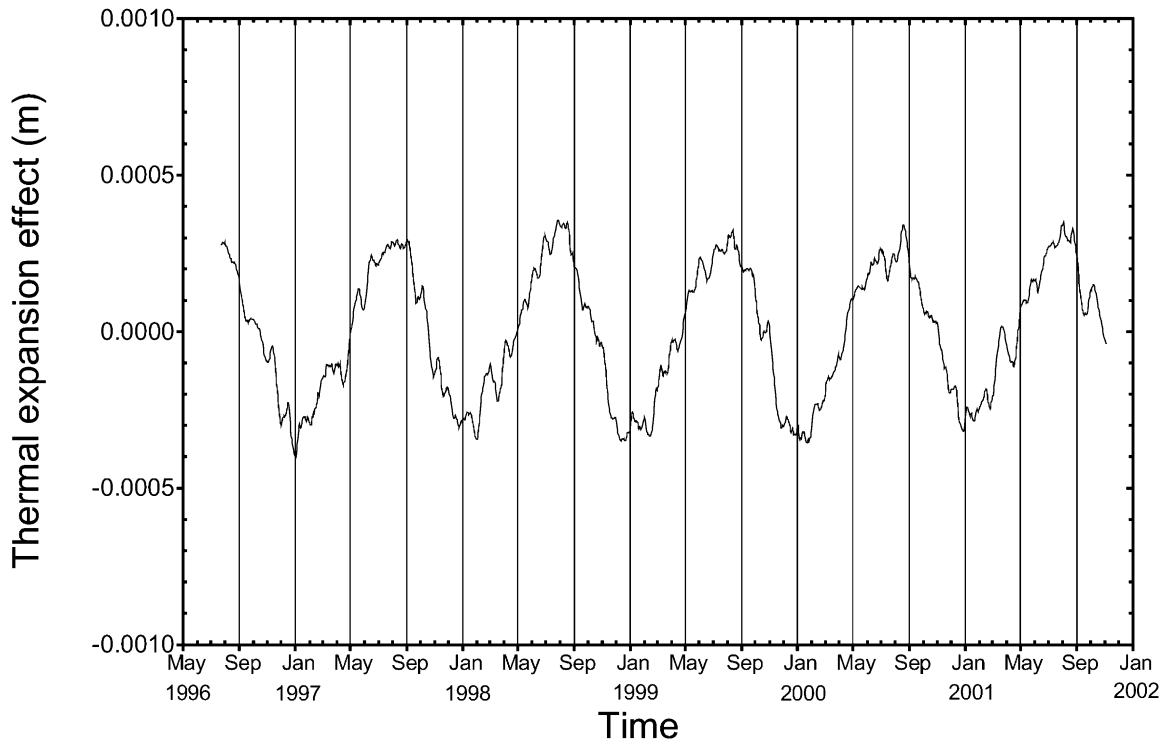


Fig. 5. Seasonal change in length of the steel pole and pillar due to the thermal expansion effect. Daily values smoothed by a 15-day window averaging.

where  $h$  is the piezometric head and  $\gamma_w$  is the unit weight of water. The effective pressure  $p'$ , which has its seat exclusively in the solid phase of the soil (Atkinson and Bransby, 1978), is given by

$$p' = h \times \gamma' \quad (4)$$

where  $\gamma'$  is the submerged unit weight of the soil, i.e. the difference between the saturated unit weight of soil and the unit weight of water ( $\gamma_w$ ). If we consider a decrease  $\Delta h$  in the water table level, the increase in the effective pressure is equal to

$$\Delta p' = \Delta h \times \gamma_w \quad (5)$$

which means that the effective pressure increase is entirely due to the lowering of the water table level.<sup>1</sup> The amount and the rate of settlement depend upon the effective pressure increase and the soil properties such as the compressibility, the permeability and the overconsolidation ratio (OCR).

<sup>1</sup> Eq. (5) is derived from (2) and (3), by assuming  $p_0' = p - u_0 = p - (h_0 \times \gamma_w)$ , where  $p_0'$  and  $u_0$  are respectively the effective and the neutral pressure relevant to the piezometric level  $h_0$ , and  $p_1' = p - u_1 = p - (h_1 \times \gamma_w)$ , where  $p_1'$  and  $u_1$  are the effective and the neutral pressure relevant to the piezometric level  $h_1$ . The effective pressure increase is  $\Delta p' = p_0' - p_1' = p - (h_0 \times \gamma_w) - p - (h_1 \times \gamma_w) = \Delta h \times \gamma_w$  as stated by Eq. (5).



#### 4.1. Stratigraphical and lithological setting of the Medicina station

The Medicina station is located in a low-lying sector of the middle Po Plain, where the surficial sedimentary sequences are mostly made up of fine-grained alluvial deposits. Detailed sub-surficial information of the area was obtained through in situ tests (Cone penetration tests CPTU) performed by the Geological Office of Regione Emilia-Romagna (Pignone, 1999), and by a specific geotechnical survey performed in the station area at the time of installation of the VLBI antenna (Montebugnoli, 1999). Quite homogeneous and compacted silty clays and clays characterize the site down to about 18 m of depth, where a coarser-grained layer was encountered, most likely composed by sand or gravelly sand. In addition, two boreholes were drilled in the first 10 m of soil, which allowed the direct stratigraphical and lithological characterization of the deposits. Main geotechnical parameters have been determined, through laboratory analyses, on five samples collected in the first 10 m of the sedimentary sequence. This data set allowed the estimation of soil consolidation effects due to seasonal fluctuations of the surficial unconfined aquifer.

The water table level is continuously monitored at the station since February 1997, in order to understand effects induced on the GPS and gravity signals. During most of the year, the water table lies quite close to the topographic surface showing maximum seasonal fluctuations in the order of 2 m. It is mainly fed by infiltration of meteoric water and less by losses in the hydrogeological surficial system. Fig. 6 shows the water table observations smoothed by a 15 day-window averaging.

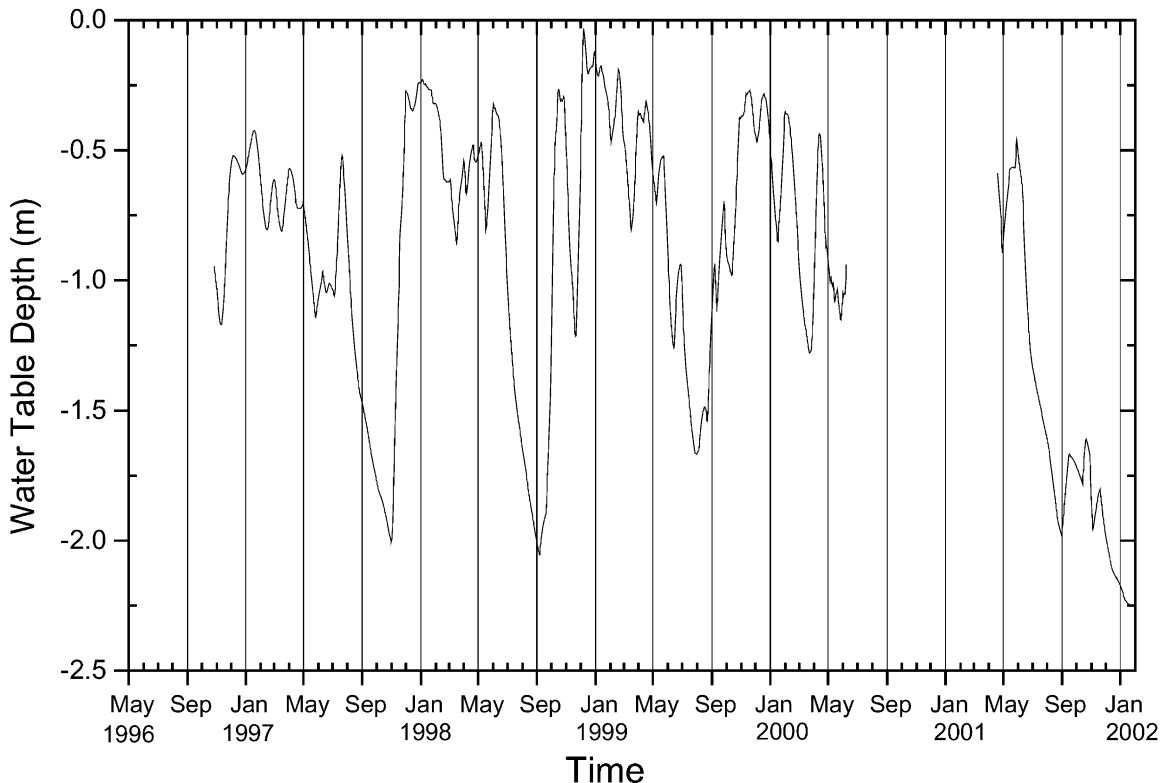


Fig. 6. Water table depth below the topographic surface smoothed by a 15-day window averaging.

Due to technical problems the water table data are missing from June 2000 to April 2001. A seasonal behavior is clearly present in the data series with minima occurring during dry seasons, which generally coincide with summer periods. The absence of any significant rainfall during the winter season in 2001–2002 has induced an unusual low level of the water table during these past few months.

The clayey soil in Medicina is characterized by low permeability, high plasticity and water retention (a consistent percentage of clayey minerals are smectites, which have a high potential for intra-crystalline water adsorption).

According to the Unified Soil Classification System (USCS), all samples are classified as CH, or high plasticity clays, with liquid limit ranging from 60% to 90% and plasticity index between 36% and 55%. The overconsolidation ratios decrease from 7.7 of the shallower sample to 1.5 of the deepest one.

Volumetric change, fabric re-arrangements and changes in the secondary permeability in the first meters of the soil may commonly occur in relation to its water content. The alternation of shrinkage on drying, and swelling on moisture uptake, is observed at the station as a seasonal effect. The lowering of the water table into the surficial sediments results in compaction due to decrease in pore pressure and to increase in effective pressures, as shown in Fig. 7. The increase in the effective pressures is calculated, according to Eq. (5), by taking into account different levels in the water table. One case,  $p'$ , refers to water table at ground surface, a second one,  $p'(-1)$ , to 1 m decrease from ground surface, and a third one,  $p'(-2)$  is relevant to 2 m decrease. The Fig. 7 also illustrates the total pressure,  $p$ , relevant to a fully saturated soil.

An estimate of the soil settlement for the Medicina station has been performed using (a) the geotechnical parameters derived by laboratory oedometric tests; (b) the cone penetration tests. Soil samples were collected in the first 10 m, at different depths, between 1–1.5, 2–2.5, 3.5–4, 7–7.5 and 9.75–10.25 m. The settlement relevant to 1 and 2 m lowering of the water table from ground surface has thus been computed down to the depth of 10 m.

For one-dimensional consolidation, as first stated by Terzaghi and Peck (1974), the soil settlement can be estimated according to the following formula:

$$s = H_0 \times C_c \times \log(p'_0 + \Delta p')/p'_0 \quad (6)$$

where  $s$  is the soil settlement,  $H_0$  is the initial thickness of the soil layer,  $C_c$  is the compression index, which can be derived by means of oedometric tests,  $p'_0$  is the initial effective pressure and  $\Delta p'$  is the increase of the effective pressure. However, a simplified approach known as the void ratio method (Capper and Cassie, 1971), based on Eq. (6), has been adopted. This method makes use of the void ratios  $e_0$  and  $e_1$ , relevant to  $p'_0$  and  $p'_1$ , respectively, which are read from the pressure/void ratio curves derived by the laboratory tests. The settlement is then computed according to

$$d \times (e_0 - e_1)/(1 - e_0) \quad (7)$$

where  $d$  is the thickness of the soil layer. In this work, 1 m thick layers have been adopted to calculate the settlement for the first 10 m of soil. Tables 1 and 2 list the values used for the computation of the settlement due to a water table lowering of 1 and 2 m, respectively.

The soil settlement effect is not the same for the GPS and gravity monuments because of the different depths of the monument foundations. The monument of the GPS antenna is founded

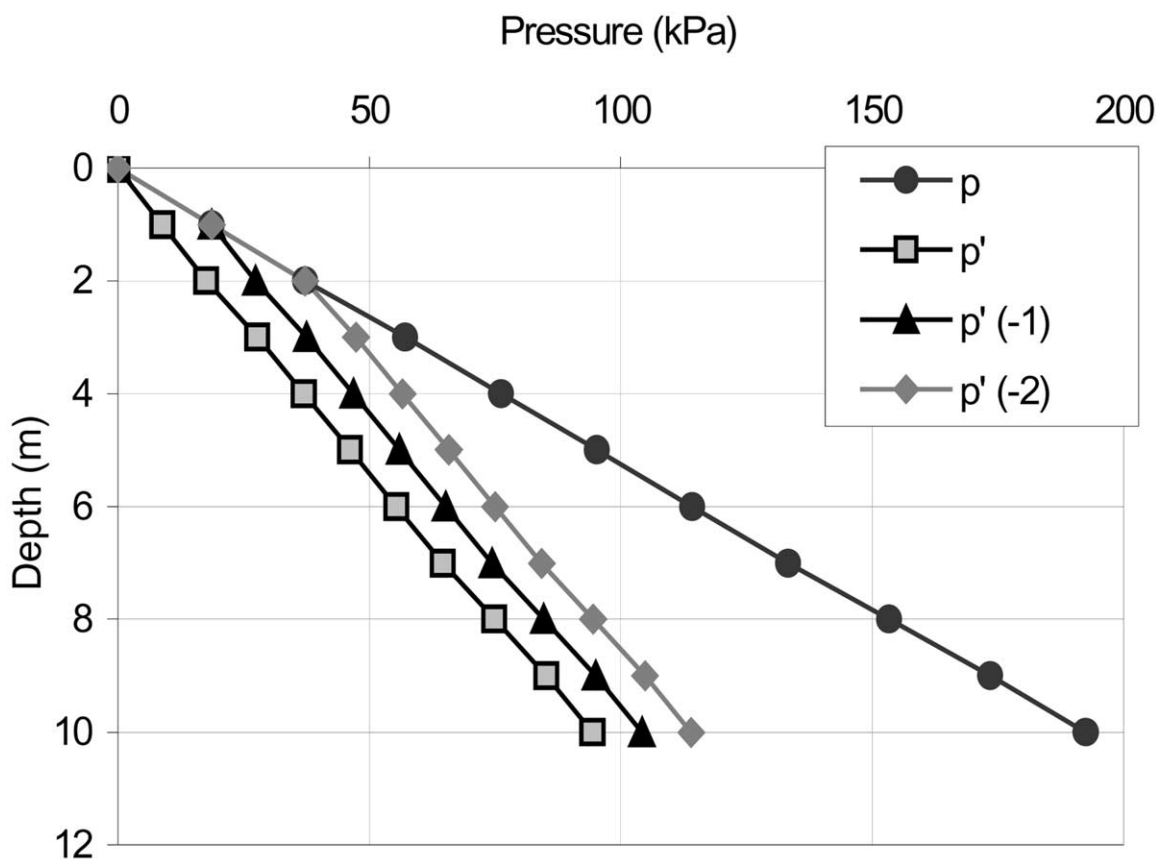


Fig. 7. Plot of the total pressure  $p$  relevant to the first 10 m of saturated soil and effective pressures  $p'$  computed for water table at ground level, at 1 and 2 m depths.

Table 1  
Computation of the settlement relevant to water table lowering of 1 m

Layer depth (m)	Initial pressure $p_0'$ (kPa)	Final pressure $p_1'$ (kPa)	Void ratio at $p_0'$ $e_0$	Void ratio at $p_1'$ $e_1$	$e_0 - e_1$	$1 - e_0$	Settlement $s$ (mm)
1–2	13.50	23.31	0.975	0.970	0.005	1.975	2.5
2–3	22.32	32.10	0.738	0.732	0.006	1.738	3.5
3–4	30.90	40.70	0.956	0.953	0.003	1.956	1.5
4–5	40.60	50.40	0.953	0.951	0.002	1.953	1.0
5–6	50.17	59.96	0.952	0.949	0.003	1.952	1.5
6–7	59.10	69.09	0.949	0.946	0.003	1.949	1.5
7–8	69.50	79.31	0.711	0.710	0.001	1.711	0.6
8–9	79.29	89.10	0.710	0.708	0.002	1.710	1.2
9–10	89.88	99.69	0.851	0.848	0.003	1.851	1.6
Total settlement							14.9

Table 2  
Computation of the settlement relevant to water table lowering of 2 m

Layer depth (m)	Initial pressure $p_0'$ (kPa)	Final pressure $p_1'$ (kPa)	Void ratio at $p_0'$ $e_0$	Void ratio at $p_1'$ $e_1$	$e_0 - e_1$	$1 - e_0$	Settlement s (mm)
1–2	13.50	27.97	0.975	0.970	0.005	1.975	2.5
2–3	22.32	41.94	0.738	0.732	0.010	1.738	5.7
3–4	30.90	50.52	0.956	0.953	0.006	1.956	3.1
4–5	40.60	60.22	0.953	0.951	0.005	1.953	2.6
5–6	50.17	69.79	0.952	0.949	0.006	1.952	3.1
6–7	59.10	78.95	0.949	0.946	0.007	1.949	3.6
7–8	69.50	89.12	0.711	0.710	0.002	1.711	1.2
8–9	79.29	98.91	0.710	0.708	0.002	1.710	1.2
9–10	89.88	109.50	0.946	0.938	0.008	1.946	4.0
Total settlement							27.0

7 m deep into the ground. Therefore it experiences only a settlement of 3.4 mm for a water table decrease of 1 m, and 6.4 mm when the water table level is at 2 m depth. Differently, the SG is installed on a concrete pier founded only 1 m deep. By taking into account the same two cases of water table lowering as for the GPS, the settlement relevant to the depth interval between 1 and 10 m turns out to be 15 and 27 mm, respectively. The total settlement for the first 10 m of soil represents quite a conservative estimate (up to a few tens percent) and it is well comparable with the settlement value obtained by using the data of the penetrometric tests. These latter ones allow the estimate of the soil settlement down to 18–20 m depth, suggesting that soil settlement below 10 m depth still occurs. However, consolidation phenomena are likely to be reduced with depth as consequence of lowering of the soil compressibility parameters and of the low hydraulic conductivity of the fine-grained soils. Data relevant to the variation of the effective pressure with depth are not available at the moment, as well as the soil geotechnical parameters for sediments in the 10–20 m depth interval. Therefore, the settlement values used for modeling the soil consolidation effect are those derived from the oedometric tests.

## 5. Loading and Newtonian attraction effects

In order to estimate the vertical displacements due to the non-tidal seasonal ocean loading, the TOPEX-Poseidon satellite altimetry data corrected for steric effects (Mangiarotti et al., 2001) were used and the Farrell's Green functions (Farrell, 1972). For the gravity data series also the seasonal mass attraction component has been estimated by means of a convolution of the ocean mass data with the Newtonian acceleration. More detailed explanation on this oceanic effect can be found in Zerbini et al. (2001). The amplitude of the annual wave describing the loading effect is in the order of 1.4 mm and maxima occur at the beginning of July. The relevant mass attraction effect is represented by an annual wave with amplitude of 0.4  $\mu\text{Gal}$  and maxima occurring in mid January.

The atmospheric loading effect on heights has been estimated by means of Green's functions modeling (Van Dam, 2002) using the NCEP global reanalysis pressure data set. The daily vertical displacements induced by the air pressure variations were then removed from the daily GPS solutions. In the case of gravity the effect of the seasonal vertical air mass redistribution shall be estimated. This is approximated by an annual wave with amplitude of  $0.8 \mu\text{Gal}$  and maxima around mid January. A detailed description of the model is given by Simon (in press).

Seasonal hydrological variations play a major role both on height and gravity variations as shown in the previous sections. In wintertime, when the water table level is in close proximity to the ground surface, the soil consolidation effects are negligible. In that season, a transfer function has been estimated between the height series and the water table to obtain the vertical displacements induced by the surficial water load variations. For example, using the data from December 1997 through May 1998 a transfer function of  $0.007 \pm 0.001 \text{ m}(\text{height})/\text{m}(\text{water})$  is obtained. This value has been used to derive the daily loading contribution of the water table. The results obtained show a peak-to-peak seasonal variation in the order of 10 mm.

The effect on gravity of both the loading and the Newtonian attraction induced by the seasonal water table fluctuations has been estimated by means of a transfer function between the gravity and the water table data series [ $4.25 \pm 0.05 \mu\text{Gal}/\text{m}(\text{water})$ ].

During the June 2000–April 2001 time frame, when the water table data are missing, the hydrological contribution was estimated by using the data of the simplified climatic hydrological balance. It has been computed (Zinoni, 2002) by taking into account precipitation and evapotranspiration data, and it turned out to be a valuable source of information when continuous water table data are not available (Zerbini et al., 2002).

## 6. Modeling seasonal height and gravity variations

The model describing height seasonal variations is obtained by summing the single modeled contributions (daily values except for the ocean loading effect) previously described. Fig. 8 shows the relevant models, which have been smoothed, for graphical purposes, by a 15-day window averaging. The only model represented by an annual wave is the one relevant to the ocean loading effect because of the seasonal temporal resolution of the available data. Major contributions to the observed seasonal oscillations come from the surficial hydrology, both in terms of loading and soil consolidation effects, and from the atmospheric pressure variations. Actually, the soil consolidation and water table loading act in opposite direction on height. The relevant effects are specular, however the loading contribution prevails. The air pressure variations are responsible for height fluctuations in the order of a few to several millimeters. The thermal expansion effect is small due to the monument characteristics and to the local climatic conditions.

Fig. 9 shows the sum of the modeled contributions, as well as the observed height series residuals (linear trend subtracted) smoothed by a 15-day window averaging. With a different symbol, for the period June 2000–April 2001, a model is presented using a simplified climatic hydrological balance instead of the water table data. In fact, the missing water table data, over this period, do not allow the computation of the soil consolidation and water table loading effects. However, the use of the climatic hydrological balance data seems to provide a satisfactory approximation of the observed height variations. One can easily notice that there are two periods during which the

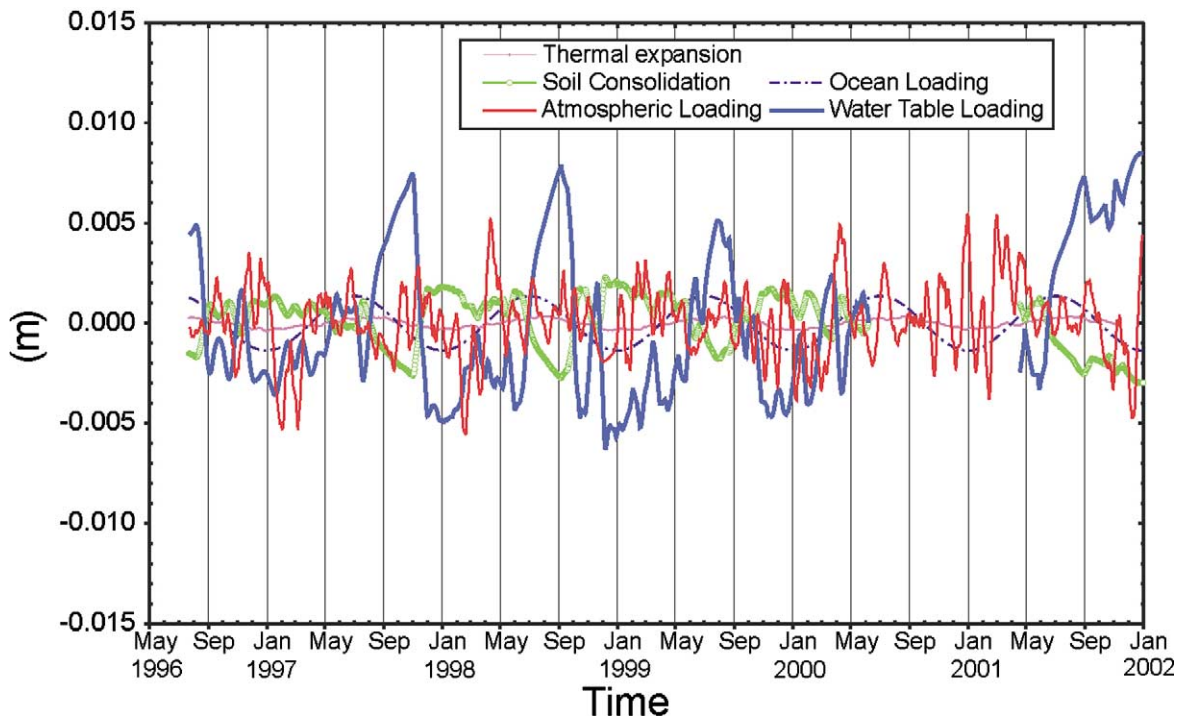


Fig. 8. Single modeled loading contributions for the observed height seasonal variations smoothed by a 15-day window averaging.

model fits the observed data less satisfactorily, namely the first one and half year after the beginning of the observations, and from mid 1999 to mid 2000. The gravity data series also show an anomaly in the August–December 1997 time frame (see Section 2.2; Zerbini et al., 2001, 2002). The differences observed from mid 1999 to mid 2000 are in the order of several millimeters. An appropriate explanation is not available till present.

Over the whole time period examined, the rms of the daily height residuals is about 6 mm while the rms of the difference between the observed and modeled height series turns out to be about 4 mm. The removal of the model thus reduces the rms of the series by 33%. During the 2-year period from mid 1997 to mid 1999, the rms of the residuals is 2.6 mm, showing the excellent agreement between the observations and the model and a reduction of 57% in the rms after removal of the modeled effects. The single modeled contributions taken into account to describe the gravity seasonal oscillations are presented in Fig. 10. Differently from the GPS modeling, in the case of gravity the air pressure variation effect is accounted for in the gravity data analysis. As previously indicated in Section 2.2, this effect is removed by means of a transfer function between the local air pressure and gravity. Therefore, it does not appear here among the components of the model. The vertical seasonal air mass redistribution effect has been estimated and is represented by an annual wave, as well as the non-tidal ocean loading and mass attraction contributions. As in the case of GPS, the surficial hydrology plays a major role both as soil consolidation and loading/mass effects. The contributions mirror each other and are in the order of several  $\mu\text{Gal}$ . The water table load/mass effect is slightly larger than the soil consolidation contribution.

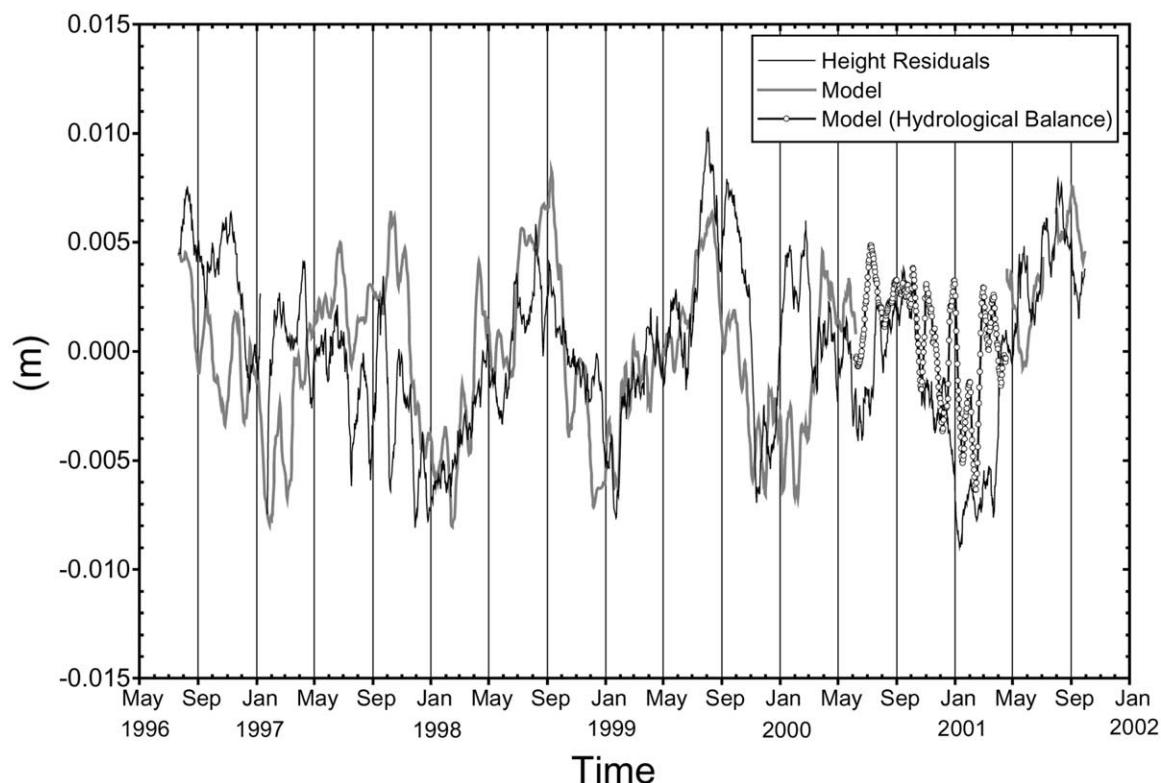


Fig. 9. Sum of all the modeled contributions and observed height residuals (linear trend removed) smoothed by a 15-day window averaging.

This latter one is relevant compared to that affecting the GPS because of the shallow foundation of the SG monument.

Fig. 11 presents the observed gravity residual variations and the sum of the different modeled contributions. Similarly to the GPS series, during the June 2000–April 2001, the model has been realized by using the simplified hydrological balance data. The model well reproduces the observed gravity seasonal oscillations. There are two clear misfits of the model, one corresponding to the period end of 1997–mid 1998, and the other in mid 2000. As regards the first, the difference is clearly attributable to the magnitude of the linear trend subtracted from the data series ( $+0.97 \pm 0.03 \mu\text{Gal}/\text{year}$ ). This is considerably smaller than the trend present in the September 1997–May 1999 time frame ( $+2.89 \pm 0.09 \mu\text{Gal}/\text{year}$ ; see also Fig. 4).

The difference between the observed gravity values and the model, occurring in mid 2000, is in the order of  $2 \mu\text{Gal}$ . At present, there is no clear explanation for this anomaly, which does not seem to be correlated with the behavior of any of the environmental parameters taken into consideration to model the seasonal oscillations.

For the September 1997–December 2001 period, the rms of the daily gravity residuals (linear trend subtracted) is  $1.6 \mu\text{Gal}$ , while the rms of the difference between the observed and modeled gravity data is  $1.1 \mu\text{Gal}$ . Removal of the model thus reduces the rms of the series by 31%. If one considers the time period July 1998–May 2000 where no significant anomalies are present in the

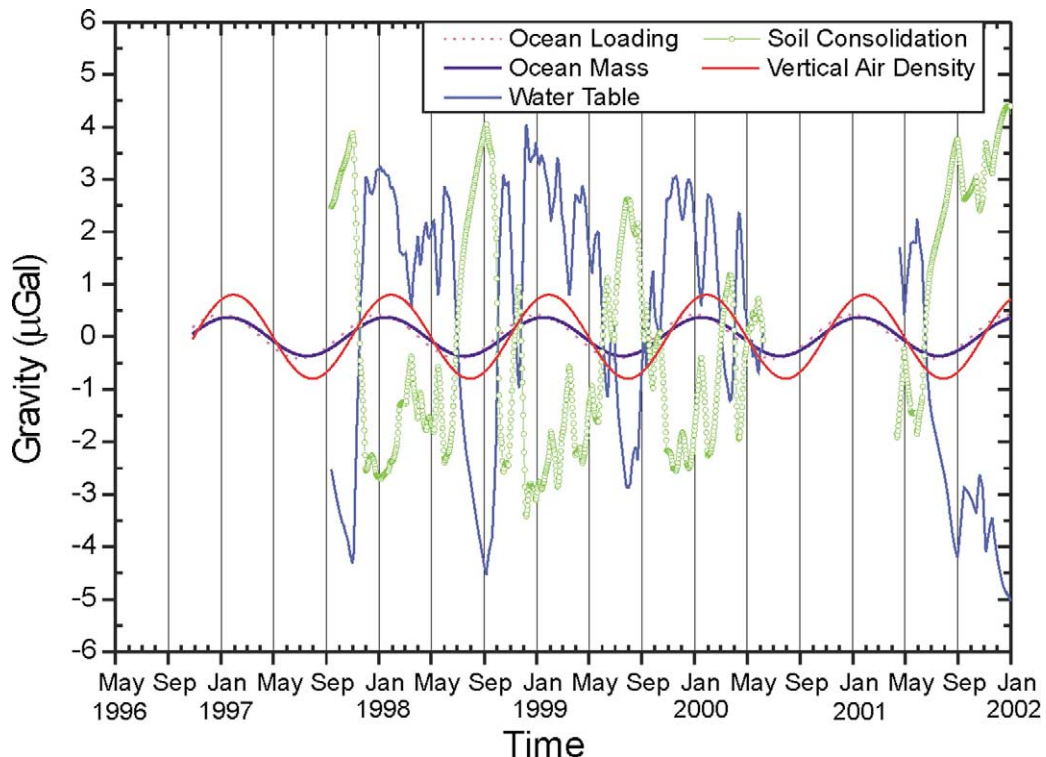


Fig. 10. Single modeled contributions for the observed gravity seasonal variations.

data, the rms of the daily gravity values turns out to be  $0.5 \mu\text{Gal}$ , corresponding to a reduction of 69% with respect to the rms of the original series.

Fig. 12 displays the difference between the observed data series and the models both for the GPS heights (a) and the gravity data (b). The rms of the residual series is quite comparable, being 4 mm for the GPS heights and  $1.1 \mu\text{Gal}$  for the gravity data. The two plots highlight the remaining unmodeled effects, which are most likely of non-seasonal nature. For example, from mid 1997 through mid 1998, the two series (plots a and b) show a similar but opposite behavior, with a difference in height up to 6 mm and a difference in gravity up to  $2 \mu\text{Gal}$  (equivalent to about 6.6 mm in the case of a pure height variation). This can be interpreted as simple height variation caused by an unknown source but without any mass redistribution.

## 7. Conclusions

The seasonal oscillations present both in the GPS heights and gravity series at Medicina have been interpreted and modeled. The models account for physical phenomena including different loadings and, in the case of gravity, also Newtonian attraction effects. In particular, in this work,



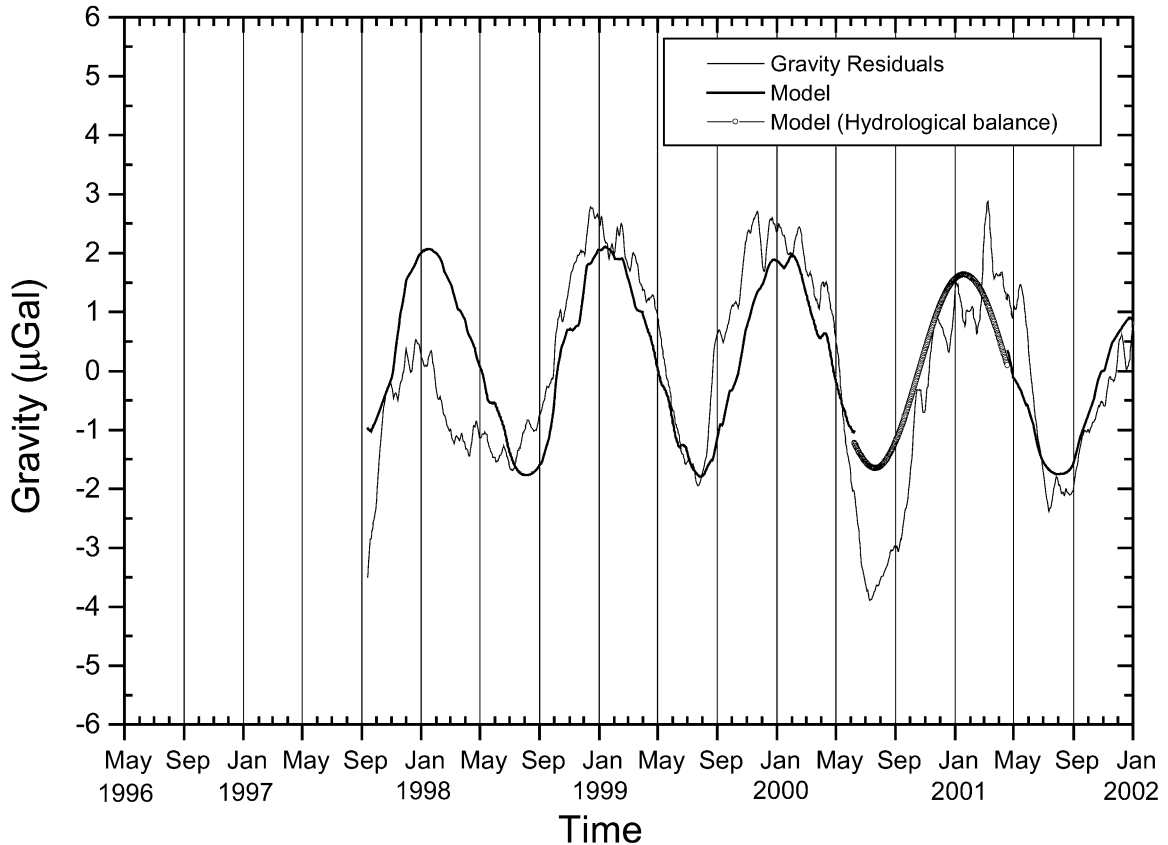


Fig. 11. Sum of the modeled contributions and observed gravity series (linear trend removed  $0.97 \pm 0.03 \mu\text{Gal}/\text{year}$ ) smoothed by a 15-day window averaging.

the contributions of soil consolidation and of thermal expansion of the pillars on which the observing systems are installed have been investigated. The clayey deposits, characteristic of this middle Plain site, favor soil consolidation processes induced by changes of effective pressures due to the water table seasonal lowering. The different foundation depths of the GPS antenna and of the SG pillars, 7 and 1 m, respectively, are responsible for significantly different soil settlements for the two observing systems. In fact, a 1 m lowering of the water table induces a soil settlement of about 4 mm for the GPS monument, while it affects by about 15 mm the SG pillar. When the water table lowers by 2 m, as it happens commonly during the summer periods, the GPS pillar experience a settlement of about 7 mm, while the SG pillar suffers a height decrease of 27 mm. It was possible to derive these estimates because of the availability of sub-surficial information obtained through in situ tests and geotechnical laboratory analyses of collected samples. These modeling results make it possible to decouple two different effects induced by the seasonal fluctuations of the surficial water table. On the one hand, a water table lowering results in a load release on the Earth's crust. On the other hand, it produces also a consolidation effect, through effective pressure increase, which is analogous to that of a load increase. In areas characterized by fine-grained soils, it is thus important to perform sub-surficial

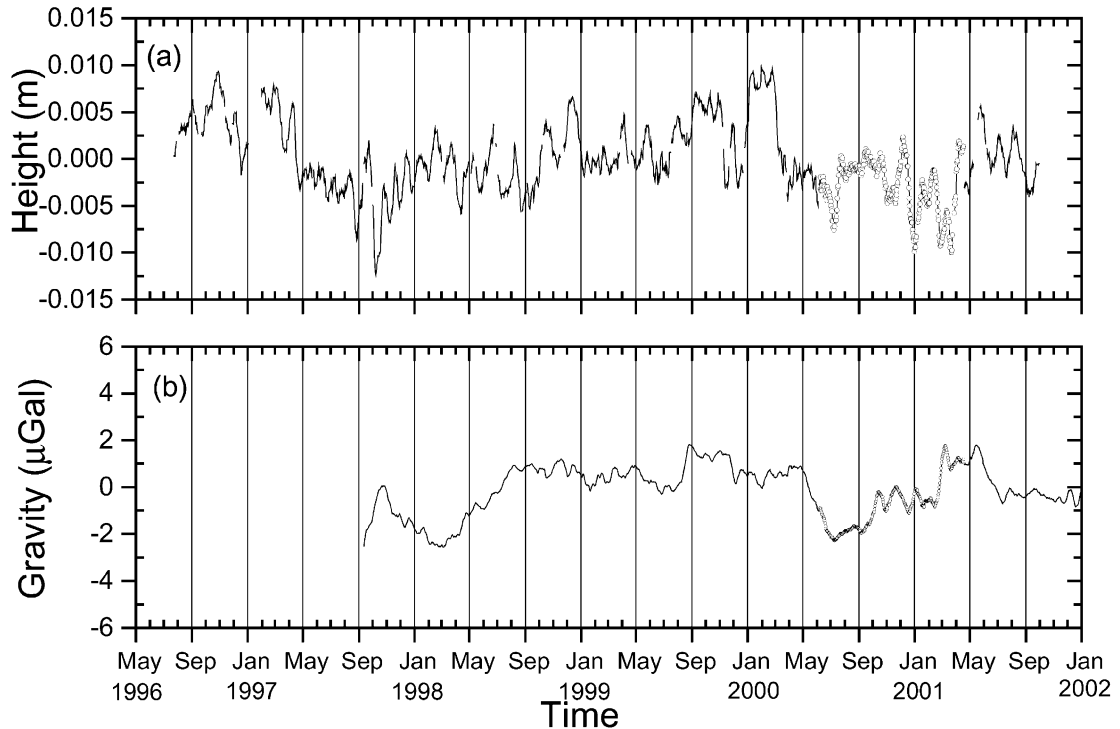


Fig. 12. Difference between the observed and modeled GPS height variations (a) and difference between the observed and modeled gravity oscillations (b). A different symbol (open circles) is used to plot the differences when the hydrological balance data have been used in the modeling procedure.

stratigraphical and geotechnical studies in order to properly understand and model seasonal height fluctuations.

The thermal expansion contribution to height seasonal variations, modeled for the GPS antenna pillar, turned out to be in the order of 1 mm. However, there are installations for which this effect might be relevant. For example, thermal expansion is significant for tall structures, such as buildings or towers, and in the case of marked seasonal temperature oscillations.

### Acknowledgements

This work has been developed under Contract I/R-144-01 from the Italian Space Agency. The NCEP Reanalysis data were obtained from the NOAA-CIRES Climate Diagnostic Center, Boulder, Colorado, at their Web site <http://www.cdc.noaa.gov>. We are grateful to the staff of the Radioastronomy Station in Medicina, in particular, S. Montebugnoli, A. Orfei and G. Maccaferri for their continuous support. We thank F. Zinoni from the ARPA Regional Agency for having provided the hydrological balance data and T. Van Dam for the atmospheric loading computations with Green's functions. R. Pignone of the Regione Emilia-Romagna Geological Office is gratefully acknowledged for having provided the cone penetration test data. We wish to thank Jacques Hinderer and an anonymous referee for their constructive suggestions.

## References

- Arca, S., Beretta, G.P., 1985. Prima sintesi geodetico-geologica sui movimenti verticali del suolo nell'Italia settentrionale. *Boll. di Geodesia e Sci. Affini* XLIV (2), 125–156.
- Atkinson, J.H., Bransby, P.L., 1978. *The mechanics of soils*. McGraw-Hill University series in Civil Engineering, McGraw-Hill Book Company, UK.
- Beutler, G., Bock, H., Brockmann, E., Dach, R., Fridez, P., Gurtner, W., Hugentobler, U., Ineichen, D., Johnson, J., Meindl, M., Mervart, L., Rothacher, M., Schaer, S., Springer, T., Weber, R., 2001. Bernese GPS Software Version 4.2. Hugentobler, U., Schaer, S., Fridez, P. (Eds.), *Astronomical Institute, University of Berne, Switzerland*, pp. 515.
- Bingley, R.M., Doodson, A.H., Penna, N.T., Teferle, F.N., Booth, S.J., Baker, T.F., 2000. Using a combination of continuous and episodic GPS data to separate crustal movements and sea level changes at tide gauges in the UK. The tenth General Assembly of the Wegener project, San Fernando, Spain, 18–20 September. Ministerio de Defensa, Real Instituto y Observatorio de la Armada, San Fernando (Cadiz), *Boletin ROA N. 3/2000*.
- Boucher, C., Altamimi, Z., Sillard, P., 1999. The 1997 International Terrestrial Reference Frame (ITRF97). Technical Note 27. Central Bureau of IERS, Observatoire de Paris, Paris.
- Capper, P.L., Cassie, W.F., 1971. *The Mechanics of engineering soils*. E.& F.N. Spon, London.
- Cremonini, S., 2002. Personal communication.
- Dong, D., Fang, P., Bock, Y., Cheng, M., Miyazaki, S., 2001. Anatomy of apparent seasonal variations from GPS derived site position time series. *EOS Trans. AGU* 82 (47). (Fall Meet. Suppl., Abstract G31A-0120).
- Farrell, W.E., 1972. Deformation of the Earth by surface loads. *Rev. of Geophys. and Space Phys.* 10 (3), 761–797.
- Mangiarotti, S., Cazenave, A., Soudarin, L., Cretaux, J.F., 2001. Annual vertical crustal motions predicted from surface mass redistribution and observed by space geodesy. *J. Geophys. Res.* 106 (B3), 4277–4291.
- Montebugnoli, S., 1999. Personal communication.
- NCEP Reanalysis data from the NOAA-CIRES Climate Diagnostic Center, Boulder, CO. Available from <http://www.cdc.noaa.gov>.
- Pignone, R., 1999. Personal communication.
- Scherneck, H.-G., Johansson, J.M., Mitrovica, J.X., Davis, J.L., 1998. The BIFROST project: GPS determined 3-D displacement rates in Fennoscandia from 800 days of continuous observations in the SWEPOS network. *Tectonophysics* 294, 305–321.
- Simon, D. The global field of gravity variations induced by the seasonal warming flash cooling of atmospheric air masses. *Cahiers du centre Européen de géodynamique et de sismologie, ECGS, Walferdange, Luxembourg* (in press).
- Terzaghi, K., Peck, R.B., 1974. *Geotecnica*. UTET, Torino.
- VanDam, T.M., 2002. Personal communication.
- VanDam, T.M., Wahr, J.M., Chao, Y., Leuliette, E., 1997. Predictions of crustal deformation and of geoid and sea-level variability caused by oceanic and atmospheric loading. *Geophys. J. Int.* 129, 507–517.
- Vauterin, P., 1998. TSoft: graphical and interactive software for the analysis of Earth Tide data. In: *Proc. 13th Int. Symp. on Earth Tides*, Brussels, Observatoire Royal de Belgique, Série Géophysique, pp. 481–486.
- Weast, R.C., Astle, M.J. (Eds.), 1982. *CRC Handbook of Chemistry and Physics*. CRC Press, Boca Raton, FL, USA.
- Wenzel, H.-G., 1998. Earth tide data processing package ETERNA 3.30: the nanogal software. In: Ducarme, B., Paquet, P. (Eds.), *Proceedings of the 13th International Symposium Earth Tides, 1997*. Brussel, pp.487–494.
- Wyatt, F.K., 1989. Displacement of surface monuments: vertical motion. *Journ. Geophys. Res.* 94 (B2), 1655–1664.
- Zerbini, S., Richter, B., Negusini, M., Romagnoli, C., Simon, D., Domenichini, F., Schwahn, W., 2001. Height and gravity variations by continuous GPS, gravity and environmental parameter observations in the southern Po plain, near Bologna, Italy, *Earth and Planet. Science Lett.* 192 (3), 267–279.
- Zerbini, S., Negusini, M., Romagnoli, C., Domenichini, F., Richter, B., Simon, D., 2002. Multi-parameter continuous observations to detect ground deformation and to study environmental variability impacts. *Global and Planetary Change* 34, 37–58.
- Zinoni, F., 2002. Personal communication.